



The anti-wear efficiency of boron succinimide on engine cylinder liner and piston ring surfaces

Doğuş Özkan¹ · Egemen Sulukan¹

Received: 15 August 2017 / Accepted: 5 November 2017 / Published online: 15 January 2018
© The Brazilian Society of Mechanical Sciences and Engineering 2018

Abstract

Anti-wear additives are important components of the lubricating oils which protect the sliding surfaces from wear. Researches on developing the non-phosphorus catalysis-friendly anti-wear additive still continue due to government's regulations. One way to provide non-phosphorus anti-wear additive is boron and sulfur addition to succinimides. In this study, boron succinimide used as an anti-wear additive is compared with ZDDPs in a real engine environment by the engine bench tests. Anti-wear performances were evaluated by microscopic and spectroscopic surface analyses on engine cylinder liner and piston rings after 100-h engine running periods for each anti-wear additive. SEM/EDX and XPS analyses were used to evaluate the tribochemical analyses of tribofilms. SEM and AFM were used to evaluate wear mechanisms on cylinder liner and piston ring surfaces. Results showed that boron succinimide can be an alternative anti-wear additive of ZDDPs from the perspective of anti-wear efficiency.

Keywords Boron succinimide · ZDDPs · Anti-wear efficiency · Tribofilm · Abrasive wear · AFM

Abbreviations

ACEA	European Automobile Manufacturers Association
AFM	Atomic force microscopy
API	American Petroleum Institute
BE	Binding energy
BDC	Bottom dead center
BN	Boron nitride
CDI	Capacitor discharge ignition
DC	Direct current
EDX	Energy-dispersive X-ray
ISO	International organization for standardization
MC	Middle center
OHV	Overhead valve
PAO	Poly-alpha-olefin
PPP-CONT	Point Probe Plus Contact

SEM	Scanning electron microscopy
Si ₃ N ₄	Silicon nitride
TDC	Top dead center
XPS	X-ray photoelectron spectroscopy
ZDDPs	Zinc dialkyldithiophosphates

List of symbols

ϑ	Viscosity Centistokes (cSt)
eV	Anode energy electron volts
h	Height millimeter (mm)
k	Nominal spring constant Newton/meter (N/m)
l	Length millimeter (mm)
N	Engine speed rotation per minute (rpm)
P	Power kilo watt (kW)
Ra_L	Cylinder liner average roughness nanometer (nm)
Ra_R	Piston ring average roughness nanometer (nm)
w	Width millimeter (mm)

Technical Editor: Jose A. dos Reis Parise.

✉ Doğuş Özkan
dozkan@dho.edu.tr
Egemen Sulukan
esulkan@dho.edu.tr

¹ Naval Academy, Mechanical Engineering Department, National Defense University, 34942 Tuzla-Istanbul, Turkey

1 Introduction

Wear is an important parameter to determine effective engine life in internal combustion engines. Especially, wear in piston ring-cylinder liner tribological system is the indicator of an effective engine life and the lifetime of this pair is related to right and quality lubricating oil usage [1]. To protect this system from the wear, anti-wear additives



HONDA GX270

Engine Type	Air-cooled, 4-Stroke, OHV, single cylinder
Bore x Stroke	77 x 58 mm
Displacement	270 cm ³
Compression Ratio	8.5 : 1
Net power	5.5 kW
Net Torque	19.1 Nm
Ignition System	Digital CDI with variable ignition timing
Lubrication System	Splash
Air Cleaner	Dual Element
Oil Capacity	1.1 L
Fuel Tank Capacity	5.3 L
Dimensions (L x W x H)	380 mm x 429 mm x 422 mm
Dry Weight	25.0 kg

Fig. 1 Specifications of the test engines

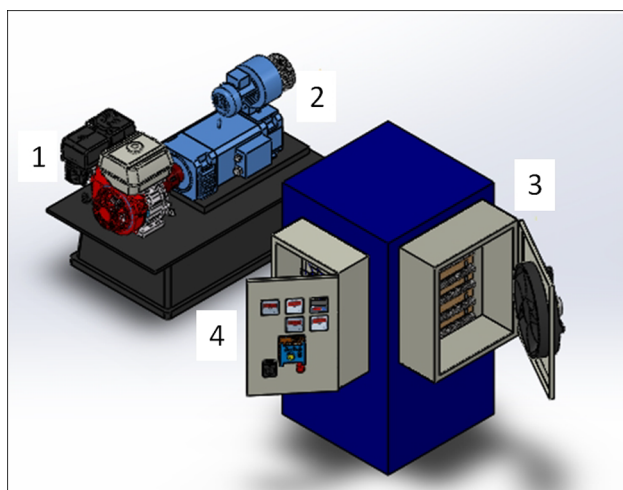


Fig. 2 Engine test bench, (1) engine, (2) DC generator, (3) electrical resistances, (4) control panel

are used in lubricating oils during the engine running conditions. The most popular and common anti-wear additive, which is used in modern fully formulated crankcase lubricants is zinc dialkyldithiophosphates (ZDDPs) that consist of sulfur (S), zinc (Zn) and phosphorus (P) elements [2]. It is mostly used due to the antioxidant properties and good performance in preventing wear for sliding pairs in engine running conditions [3]. In addition to this, ZDDPs has been a cost-effective and proven technology for internal combustion engines for recent 30 years [4, 5]. Decomposition of this additive under load and heat forms a tribofilm on sliding surfaces which protects surfaces from wear. The ZDDP-derived tribofilm contains metal sulfates and sulfides, Oxygen (O), P and Zn compounds in its typical composition [6]. However, it contains

P, Zn and S elements, which are hazardous for environment and these elements have a poisoning effect on the engine catalysis [7, 8]. Especially, Zn and P, which produce glassy zinc phosphate layers on wash coat surfaces, block the pores of the engine catalysis. Therefore, catalysis' efficiency of the vehicle is reduced and emissions increase [9–11]. In addition to this, latest regulations which were implemented by American Petroleum Institute (API) in 2010 and European Automobile Manufacturers Association (ACEA) in 2012 decreased S and P concentrations in lubricating oils due to their negative environmental effects [12, 13]. Furthermore, these legislations will tend to decrease S and P concentrations more or even remove these elements from the lubricating oils in the near future. Requirement to ensure the durability of engine catalysis, hence maintain exhaust emission standards and legislation restrictions, have led to a demand for crankcase lubricants, which contain reduced levels of Zn, S and P [14, 15]. As a result, lubricating oil manufacturers and researchers have been working on removing or reducing this content in lubricating oils. One way to provide the non-ZDDPs anti-wear additive is the use of succinimides, which are chemical compounds, composed of long-chain carbon and hydrogen atoms. An alternative anti-wear additive candidate can be evaluated by adding S and boron to succinimides [16–19]. This novel study presents the anti-wear efficiency of two additive package by detailed, quantitative topographical (wear phenomena was investigated in great detail) and tribochemical analysis by SEM, XPS and AFM which were run in real engine environment. In this study, the anti-wear performance of disulfide, nitrogen-containing boron succinimide additive package has been evaluated and compared to ZDDP additive package in piston ring–

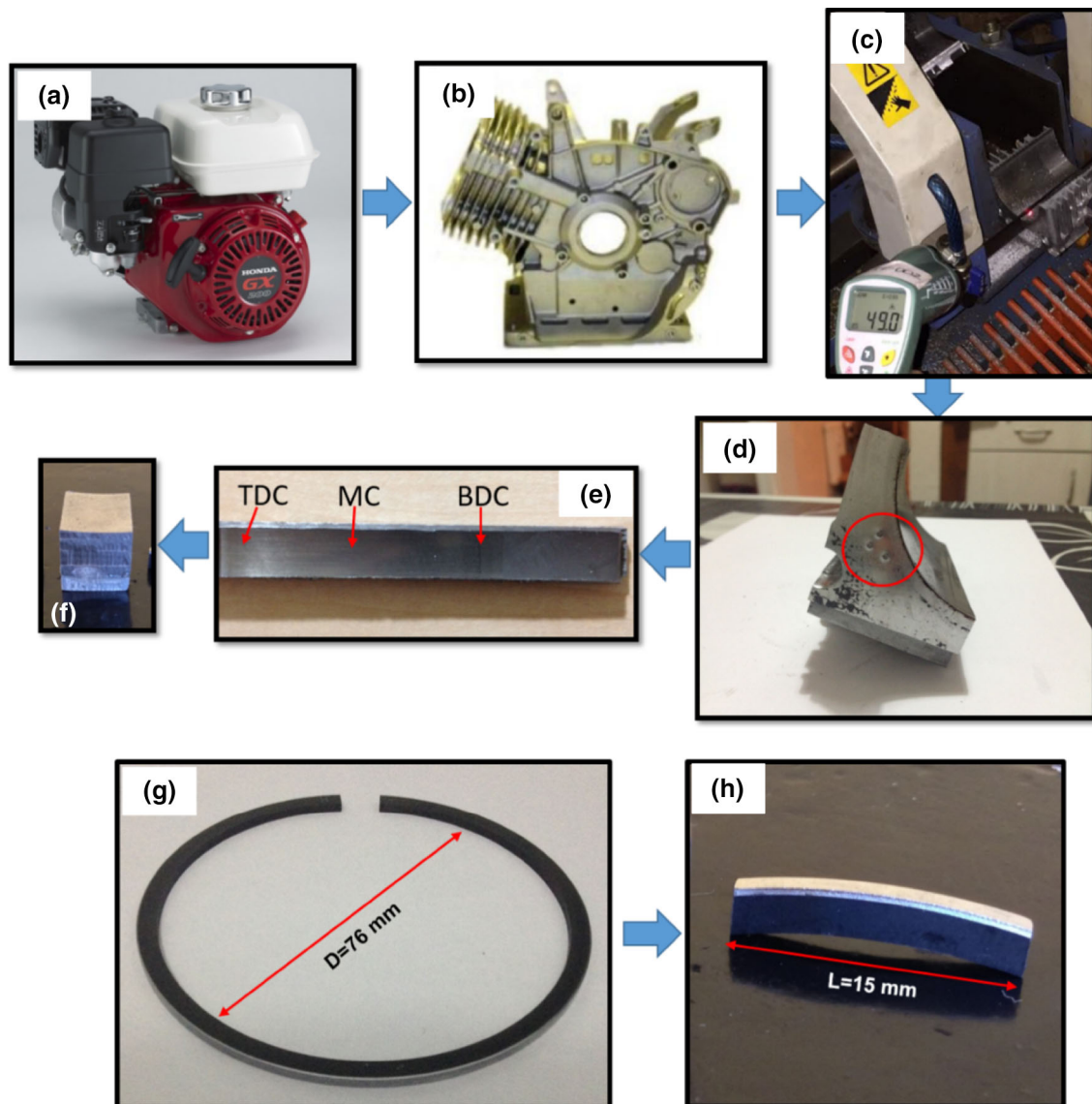


Fig. 3 Engine cylinder liner and ring sample preparations at the end of the 100-h tests, **a–f** cylinder liner sample preparation, **g, h** piston ring sample preparation

cylinder liner tribological system using engine bench tests. To find out whether S- and B- containing succinimide can be alternative anti-wear additive or not, the anti-wear performances of these packages were studied by chemical analyses of tribofilm formations and wear analyses of the engine piston rings and cylinder liners at the end of 100-h engine bench tests. Wear mechanisms were evaluated by scanning electron microscopy (SEM) and atomic force microscopy (AFM). Especially, AFM was used in quantitative wear scar and tribofilm characterization where optical profilometers are not suitable for curved cylinder liner and piston ring surfaces. Chemical analyses of tribofilms were investigated by energy-dispersive X-ray spectroscopy (EDX) and X-ray photoelectron spectroscopy (XPS) techniques. Results showed that sulfur- and boron-

containing succinimide can be used as an alternative anti-wear additive of ZDDPs to protect piston ring–cylinder liner tribological system from the wear in engine running conditions.

2 Materials and methods

2.1 Lubricating oil and additive preparation

Synthetic poly-alpha-olefin (PAO) [viscosity (ν) with 14.6 cSt @100 °C] was used in all experiments as base oil. The ZDDP-containing lubricating oil includes 0.09 wt% Zn, 0.20 wt% S and 0.09 wt% P. Succinimide consisted of 0.16 (wt%) boron, a disulfide compound as a component

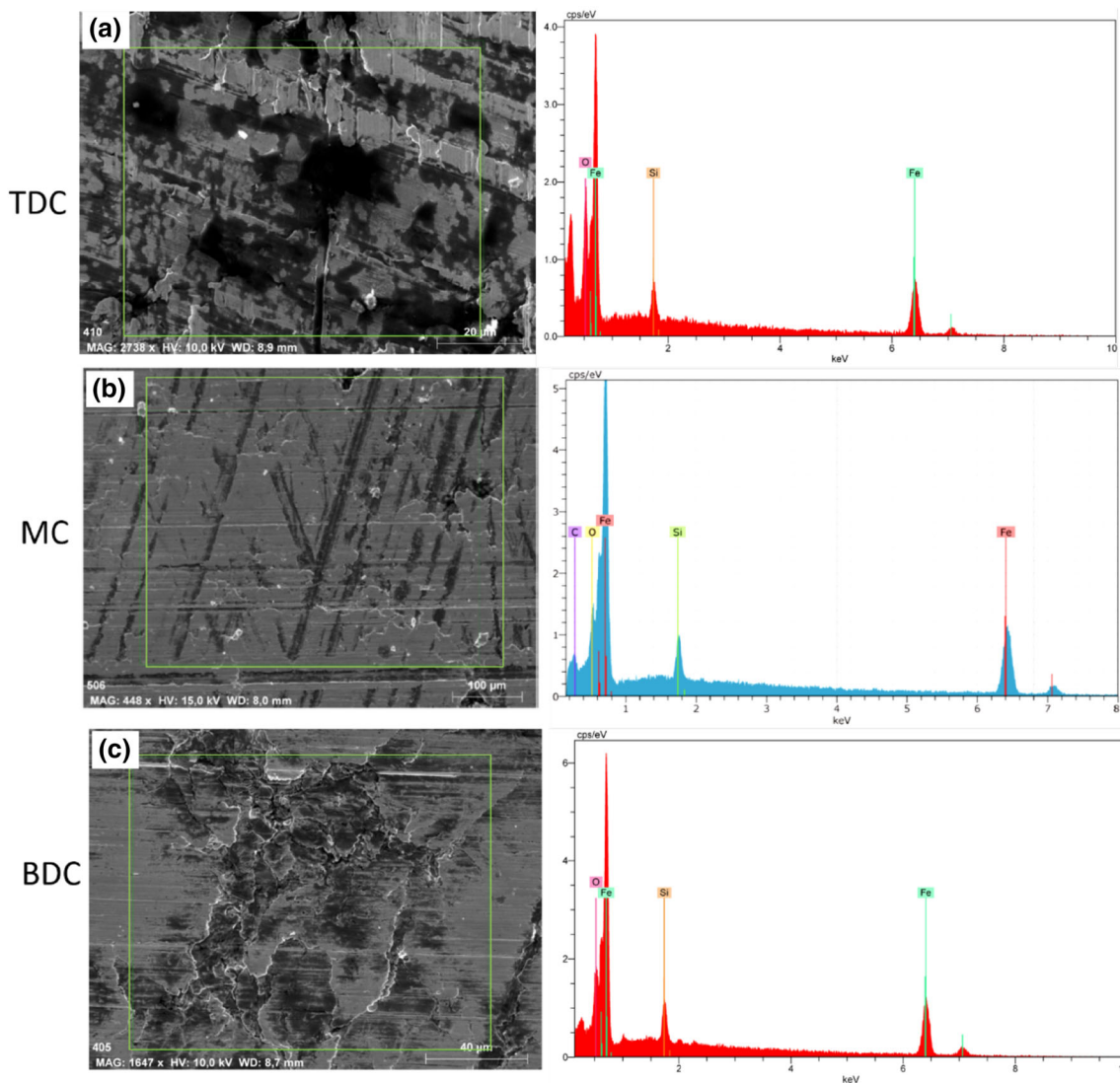


Fig. 4 SEM/EDX analyses of engine cylinder liner run with boron succinimide anti-wear additive

containing 0.26 sulfur (wt%) and 0.41 N (wt%). Nitrogen was used to make boron- and disulfide-containing compound hydrolytically more stable by donating a lone pair of electrons to boron.

2.2 Two new test setup and test conditions

Honda GX-270, single-cylinder, air-cooled engines with 1.1 L lubricating oil capacity were used in the tests. Engines ran one oil drain period, which corresponded to 100 h. Figure 1 shows the test engine and its technical specifications. The engine bench was constructed in our laboratory and it consisted of the engine, a DC generator for electrical resistances and control panel as shown in Fig. 2.

The engines ran 100 h with 50% of maximum load which corresponded to 2.5 kW power (P) and 2500 rpm

speed (N) as indicated in ISO 8178-4 (Reciprocating internal combustion engines—Exhaust emission, Part 4: Steady-state test cycles for different engine application measurement) standard. Tests were carried out at 25 °C ambient temperature and 65% relative humidity.

2.3 Characterization of the piston rings and cylinder liner

Mechanical parameters are important for rubbing surfaces to study wear mechanisms. Therefore, mechanical characterizations (hardness and Young's modulus) of unused engine cylinder liner and piston rings were evaluated by nanoindentation. Surface roughness of the liner and ring samples were measured by AFM, which could provide delicate results. Engine cylinder liner was gray cast iron with 3.25 GPa hardness and 125 GPa Young's modulus.

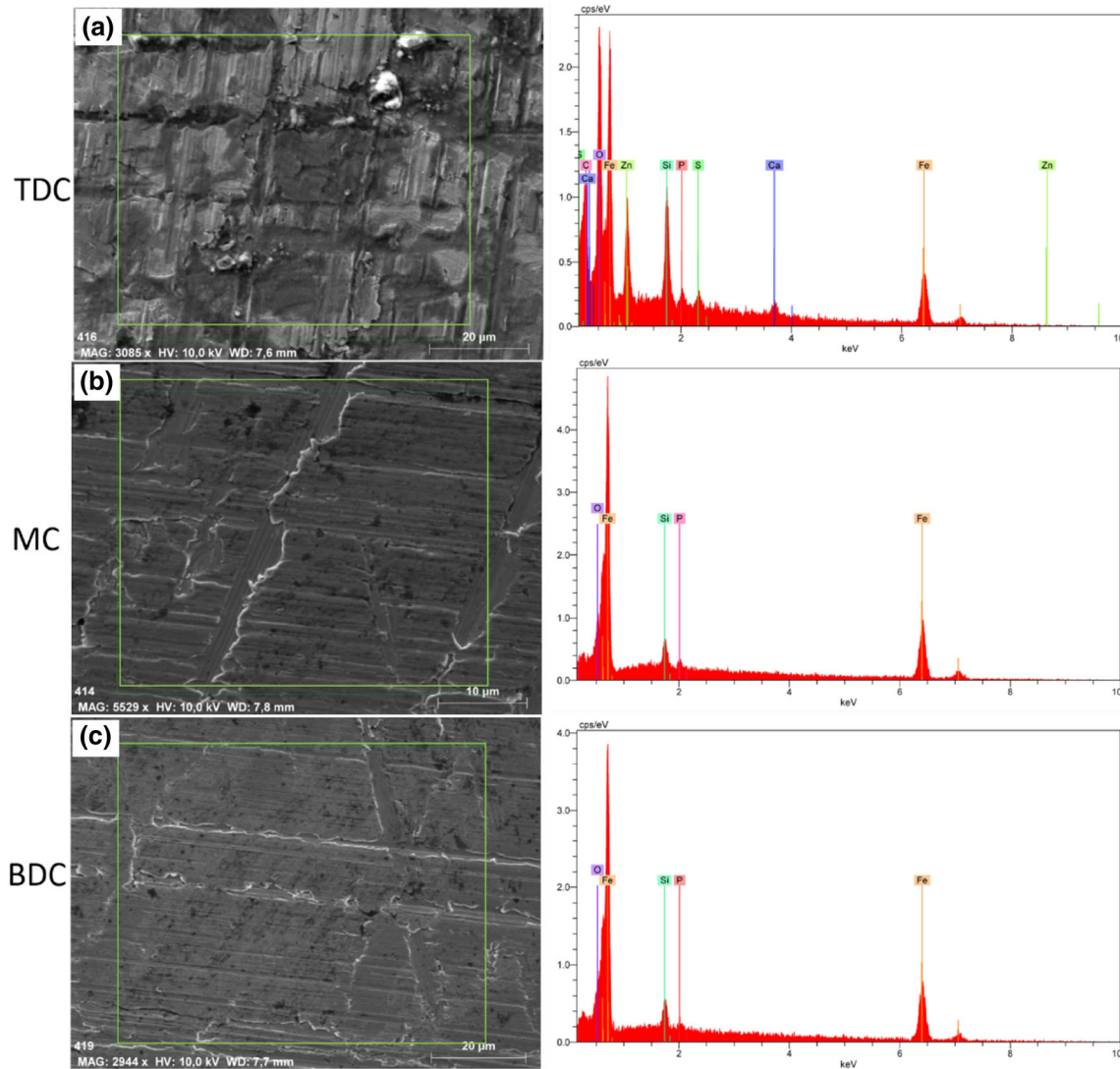


Fig. 5 SEM/EDX analyses of cylinder liner run with ZDDP anti-wear additive

The typical elemental composition was 93.95% Fe, 3% C, 0.3% P, 0.15% V, 0.6% Mn and 2% Si by weight. Average roughness was measured as $Ra_L = 273$ nm. Top compression ring was chromium-coated spheroidal graphite cast iron. The thickness of the chromium coating was 100 μm , measured by SEM, the hardness 16 GPa, Young's modulus 275 GPa and average roughness $Ra_R = 162$ nm.

2.4 Sample preparation

After 100 h of engine running, the engine cylinder heads were dismantled, cylinders were divided into four sections and marked as seen in Fig. 3d and identified by the red circle. Similarly, piston ring faces were numbered with the same number of cylinder liner sections. Samples from top dead center (TDC), middle center (MC) and bottom dead center (BDC) liner sections were cut into

9.5 mm \times 12 mm \times 8 mm ($w \times l \times h$) for microscopic examinations as seen in Fig. 3f. The specimens were cut by dry cutting method with horizontal band saw in very low speed. It is considered that the substrate temperature was controlled during the cutting process due to the possible material property changes and to not destroy or change any formed tribofilm at cylinder liner substrates induced by heat. Substrate temperature was monitored during the cutting process by digital infrared thermometer and did not exceed 49 $^{\circ}\text{C}$ (Fig. 3c). Test substrates had been cleaned ultrasonically with heptane for 5 min and then dried before surface examinations.

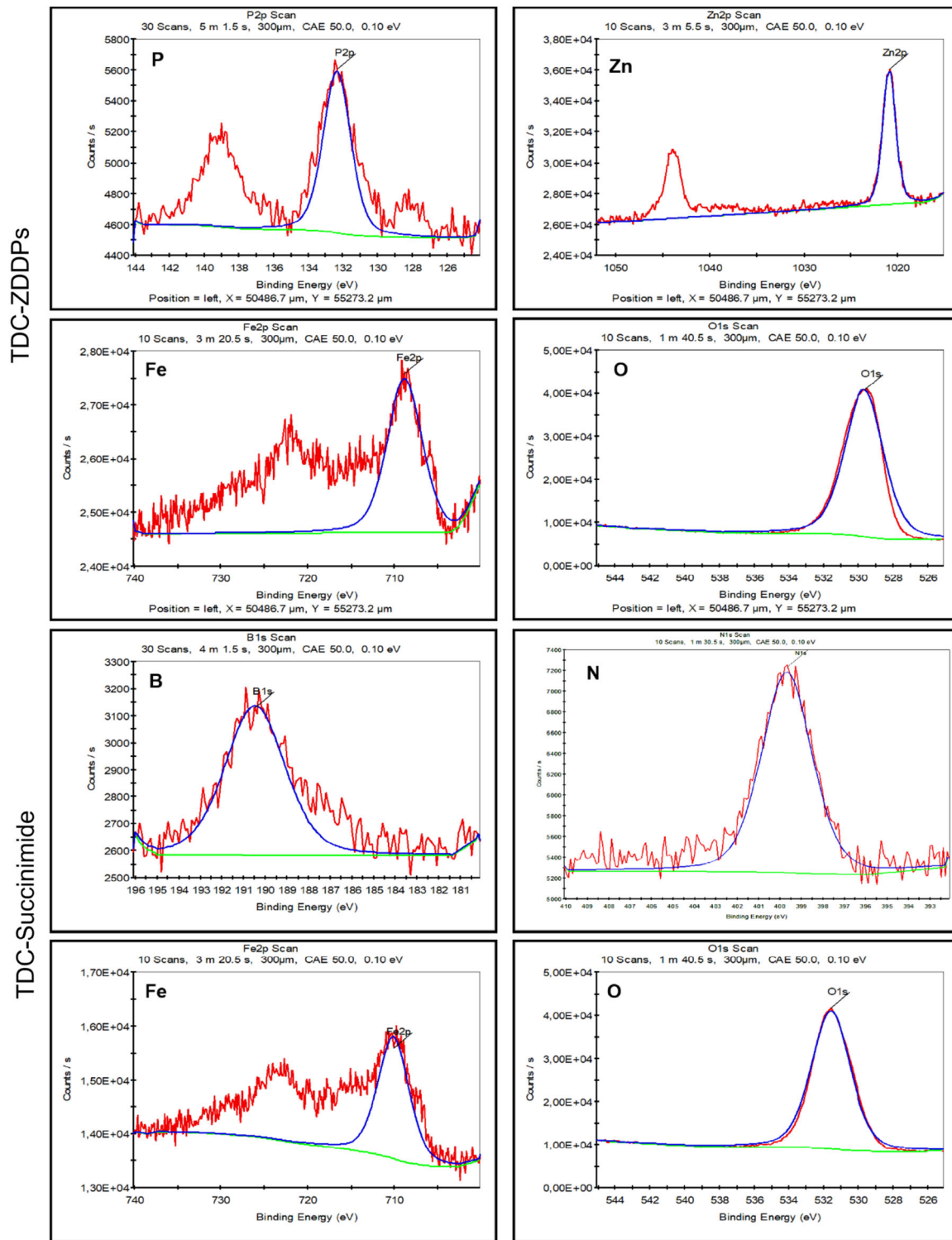


Fig. 6 XPS analyses on TDC surfaces of cylinder liners

2.5 Surface and tribochemical analyses of cylinder liner and ring samples

FE-SEM was employed to detect wear mechanisms, topographic changes and measure wear scar widths. AFM

contact mode was used to evaluate the tribofilm formations, topographical changes and to measure wear scar width and depth. Point Probe Plus Contact (PPP-CONT), uncoated silicon nitride (Si_3N_4) cantilever (width = 46 μm , length = 452 μm , nominal spring constant, $k = 0.081 \text{ N/}$

Table 1 XPS analysis results of the cylinder liner surfaces run with boron succinimide-containing lubricating oil

Engine liner	TDC			MC			BDC		
	Peak BE	Atomic %	Compound	Peak BE	Atomic %	Compound	Peak BE	Atomic %	Compound
B1s	190.8	7.55	BN	191.8	3.34	BN–O	190.9	2.77	BN
C1s	284.7	62.56	C–C	284.9	53.95	C–O	284.2	19.2	C–C
N1s	399.5	3.76	B–N	399.3	3.56	B–N	398.5	2.29	C–N
O1s	531.2	20.94	C–O	531.3	27.43	C–O	529.9	44.21	Mn–O
Fe2p	710.3	5.19	Fe ₃ O ₄	710.9	8.19	Fe ₂ O ₃	709.5	25.84	FeO

Table 2 XPS analysis results of the cylinder liner surfaces run with ZDDP-containing lubricating oil

Engine liner	TDC			MC			BDC		
	Peak BE	Atomic %	Compound	Peak BE	Atomic %	Compound	Peak BE	Atomic %	Compound
P2p	134.2	2.47	ZnP	139.1	1.62	P–O	139.9	1.81	P–O
C1s	284.2	49	C–C	283.8	23.07	C–C	285.4	22.13	C–O
S2p	169.0	0.32	SO ₄	168.4	0.39	FeSO ₄	–	–	–
O1s	531.5	28.85	ZnP	530.5	47.61	C–OH	531.5	41.56	ZnP
Fe2p	710.0	0.78	Fe ₃ O ₄	709.4	7.38	Fe ₂ O ₄	710.9	20.54	FeO
Zn2p	1021.8	1.86	ZnO	1021.3	1.9	ZnO	1022.4	1.71	Zn ₂ O

BE binding energy

Table 3 XPS analysis results of the ring surfaces run with boron succinimide-containing lubricating oil

Engine piston rings with boron succinimide				Second compression ring (uncoated)		
	Peak BE	Atomic %	Compound	Peak BE	Atomic %	Compound
B1s	190.7	5.70	BN	190.6	3.83	BN
C1s	283.9	33.39	C–C	283.9	23.07	C–C
O1s	529.5	28.85	N–O	530.5	47.61	C–OH
Fe2p	708.9	4.46	Fe ₂ O ₃	709.4	7.38	Fe ₂ O ₄

Table 4 XPS analysis results of the ring surfaces run with ZDDP-containing lubricating oil

Engine piston rings with ZDDPs	First compression ring (Cr coated)			Second compression ring (uncoated)		
	Peak BE	Atomic %	Compound	Peak BE	Atomic %	Compound
P2p	132.3	1.23	PO ₄	132.3	1.58	PO ₄
Zn2p	1020.8	0.85	Zn–O	1020.7	0.68	Zn–O
Fe2p	708.8	1.23	FeO	708.6	18.9	Fe ₂ O
S2p	160.8	0.73	S–S	160.9	0.48	S–S

m) was used in all AFM measurements. First, topographic images of each wear scar were taken with a $90 \times 90 \mu\text{m}^2$ scan size and then focused on each detected wear scar by

performing depth and width measurements. Various locations and numerous scans (25–30 scans) were studied to get statistically representative results. AFM scan head delivers

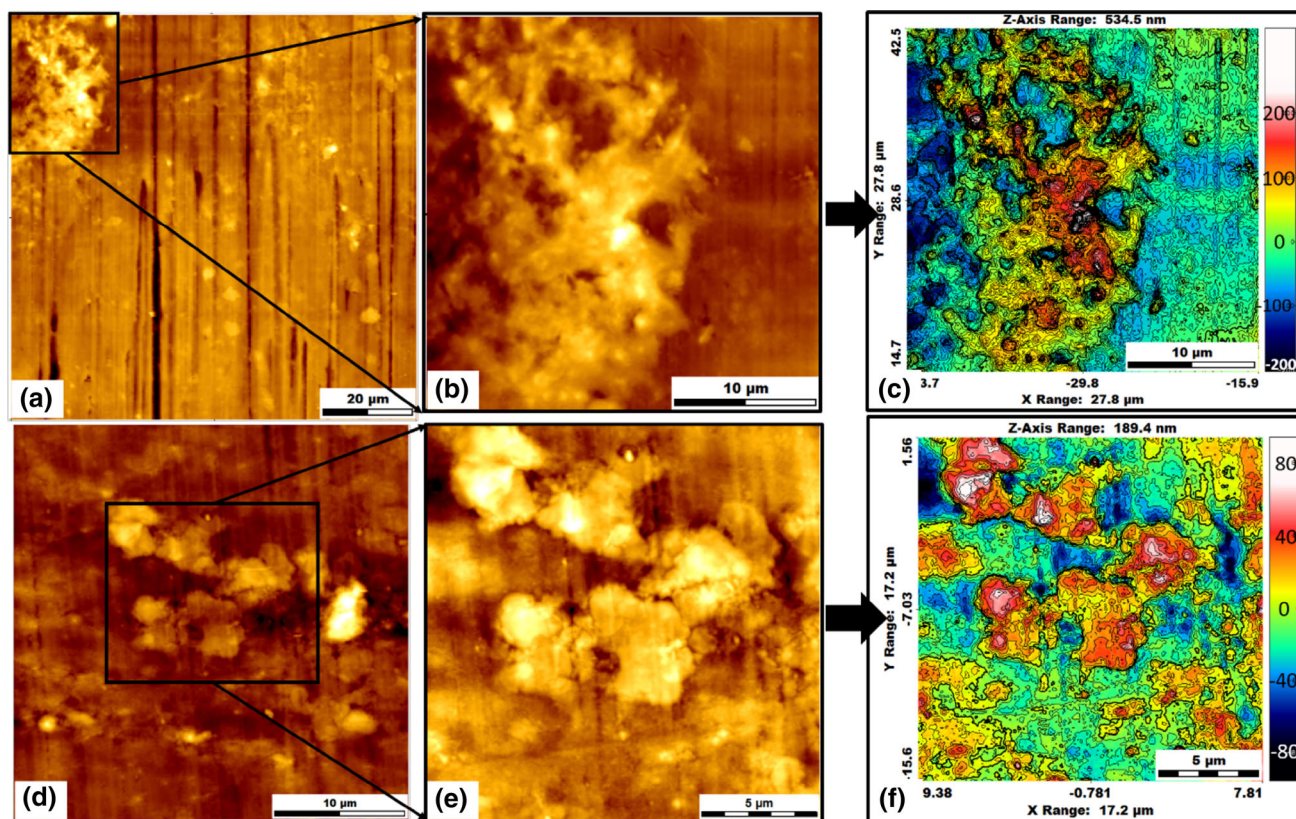


Fig. 7 AFM analyses of tribofilms formed on chromium-coated piston rings, **a** tribofilm formed by ZDDPs, **b** tribofilm formed by succinimide anti-wear additive

an average linearity deviation of less than 0.1% over the full scan range, as declared by Nanosurf Company, for the wear scar width and depth measurements. Uncertainty rate was 0.1% for the wear scar and depth measurements. EDX was applied to the substrate surfaces for elemental analyses and XPS with 1468.3 eV anode was used to determine tribochemical compounds of the tribofilms formed by the lubricating oil anti-wear additives.

3 Results and discussion

3.1 Tribofilm formation

SEM/EDX analyses were performed as an area search for elements of anti-wear additives. Figure 4 shows engine cylinder liner SEM/EDX analysis results of TDC, MC and BDC sections which were run with boron succinimide-containing lubricating oil. Si, Fe, C, O elements were detected and no boron element was detected on both the surfaces as it can be seen from the EDX spectra. When looking at cylinder liner sections run with ZDDP-containing lubricating oil (see Fig. 5), Zn, P and S were found in the tribofilm, formed by the decomposition of the ZDDPs.

In addition to this, Zn, P and S were most densely distributed at TDC, while they were very low at the MC and BDC. This can be explained by thermal decomposition of the ZDDPs under higher level of temperatures and loads at TDC when compared to MC and BDC in the engine. Similarly, Gosvami et al. reported that this situation was a result of ZDDP decomposition and tribofilm formation increases exponentially with the load and temperature where these are in higher level at TDC [19]. It is not easy to detect boron with EDX analysis. The acceleration voltage of EDX was decreased to 5, 3 and 1 kV to detect boron on the surfaces. However, it was not able to detect boron on the surfaces. Therefore, XPS surveys were performed for detailed tribofilm analyses.

XPS analysis results (see Fig. 6) of engine cylinder liners showed that boron succinimide-containing lubricant formed boron nitride anti-wear tribolayers by boron nitrogen reaction on both TDC, MC and BDC surfaces of cylinder liners (see Table 1). The electronic structure of boron which has three electrons in the valence shell easily provides covalent bonds with the non-pair bonding electron of nitrogen which carried out boron nitride (BN) tribo-compound during the sliding process [20, 21]. The determined quantity of boron in the tribofilm was the highest at

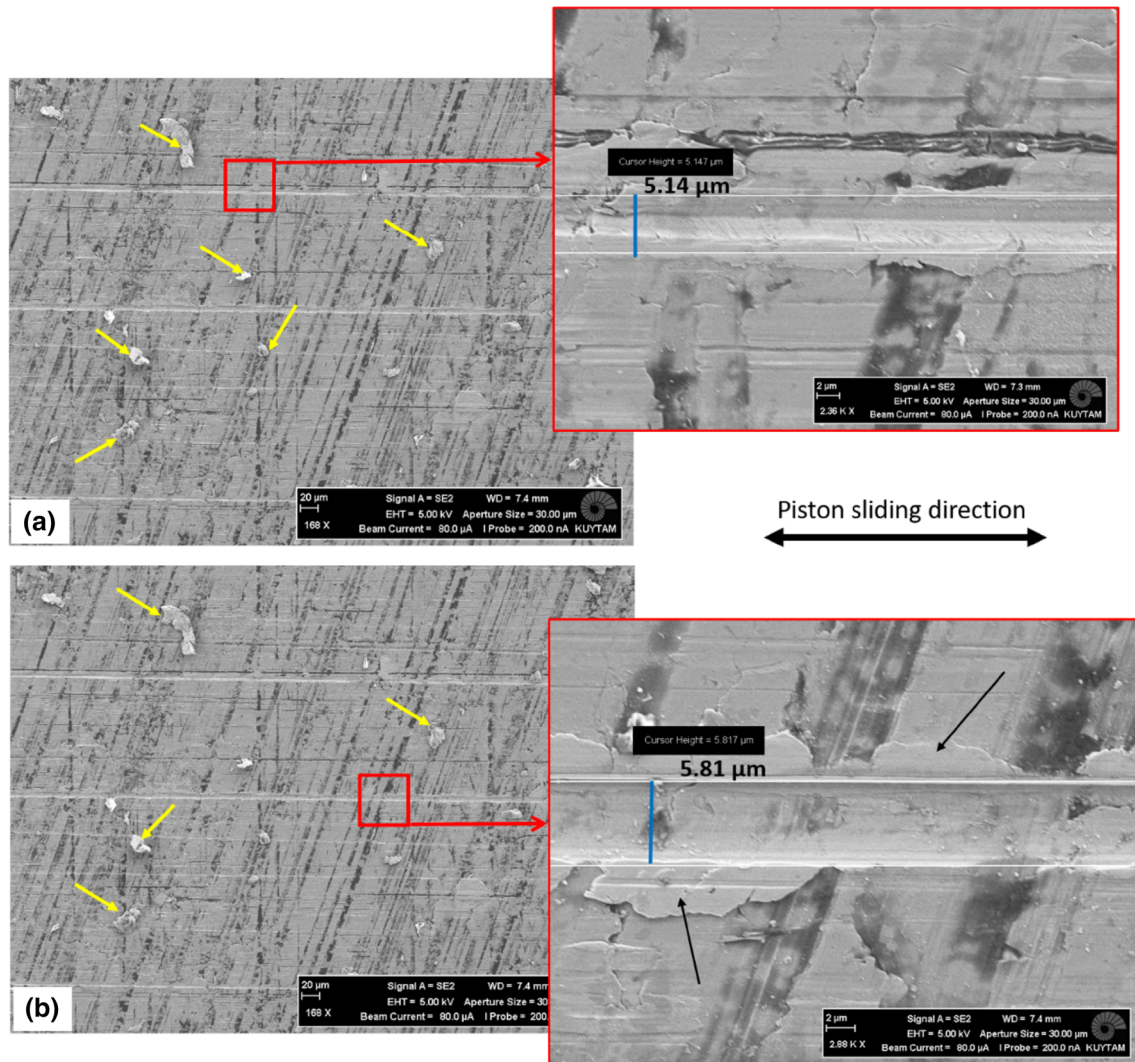


Fig. 8 Abrasion wear analyses at TDC of the cylinder liner surface run with boron succinimide, **a** cutting type abrasive wear and yellow arrows point out wear debris, **b** ploughing type abrasive wear and removed material from grove to ridges is shown with black arrow (color figure online)

TDC and the lowest at BDC (see Table 1). Similar to EDX results of ZDDPs, higher temperatures and contact pressures at TDC accelerated and increased the decomposition of boron in succinimide. This provided higher level of boron or chemical boron compound deposition in the tribofilms, which formed at TDC surface [22]. The XPS survey results in Table 2 show zinc oxide, phosphate and organic sulfide species on the tribofilm formed on the gray cast iron cylinder liner surface after 100 h, confirming rapid tribofilm formation as a result of ZDDP decomposition. The dominant anti-wear tribolayer was zinc polyphosphate films at TDC due to the higher reactivity of ZDDPs with the surface because of the presence of phosphate moiety. According to the XPS results in Table 2, iron sulfate, PO and ZnO chemical compounds were detected at MC, which run with ZDDPs. Similar to the literature findings, ZnO and PO chemical bonds and ZnP layers,

which provide anti-wear efficiency were detected on the tribofilm at BDC surface [23, 24]. When looking at piston rings, similar results were obtained on the compression ring running surfaces, which run with boron succinimide anti-wear additive. BN anti-wear layers formed on both ring surfaces (see Table 3). PO and ZnO chemical compounds were observed on the tribofilm due to decomposition of ZDDPs on compression rings (see Table 4). However, more iron, which indicates wear transfer element, was detected on chromium-coated piston ring surface run with boron succinimide additive than run with ZDDPs additive.

The thicknesses of the tribofilms formed on the piston rings were measured and mapped by AFM (see Fig. 7). Both tribofilms formed pads of different thicknesses on the surfaces. The tribofilm thickness formed by boron succinimide changed from 80 to 130 nm as shown in Fig. 7c and the tribofilm thickness formed by ZDDPs changed from 40

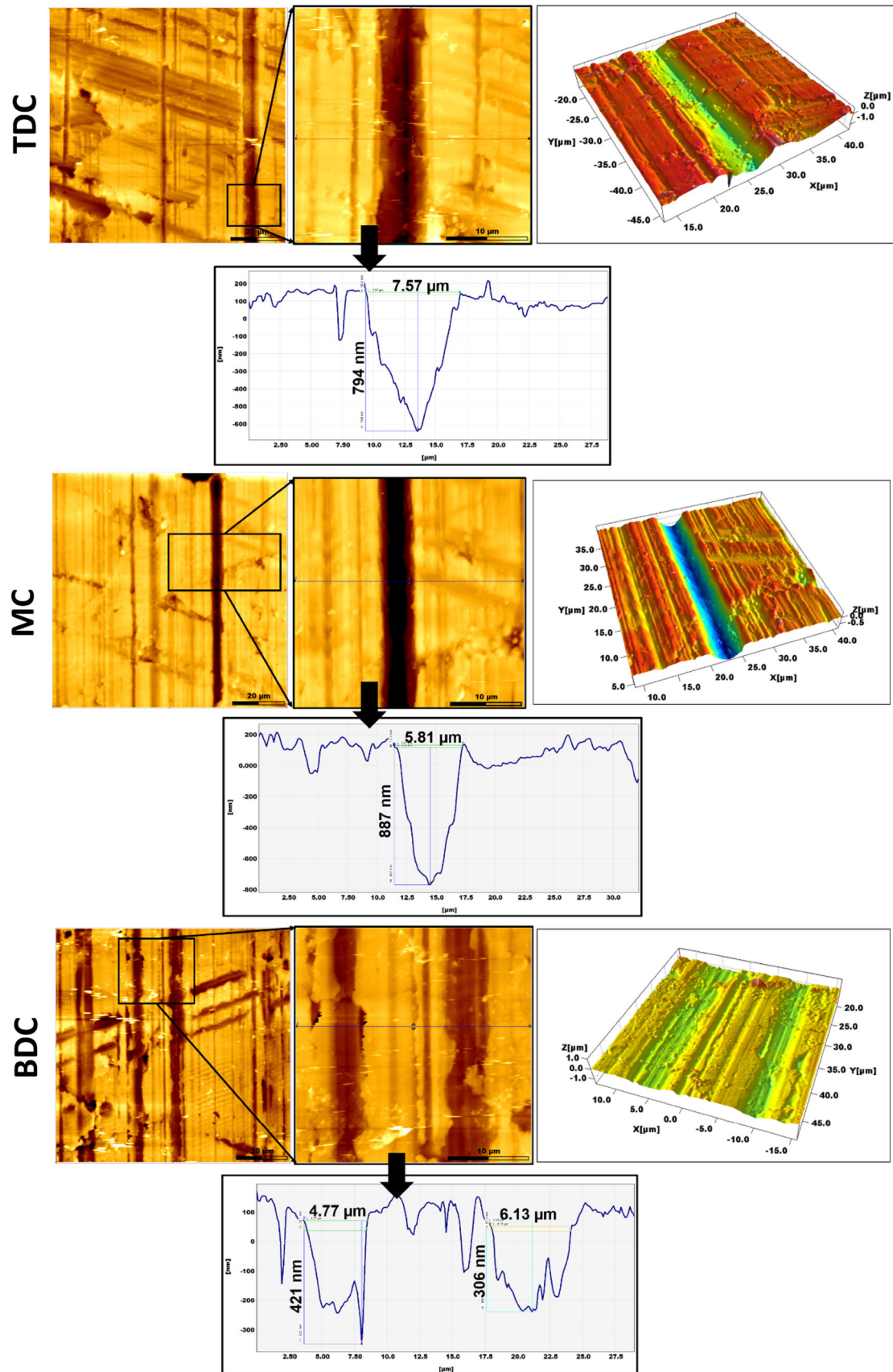


Fig. 9 AFM analysis on cylinder liner surface run with boron succinimide

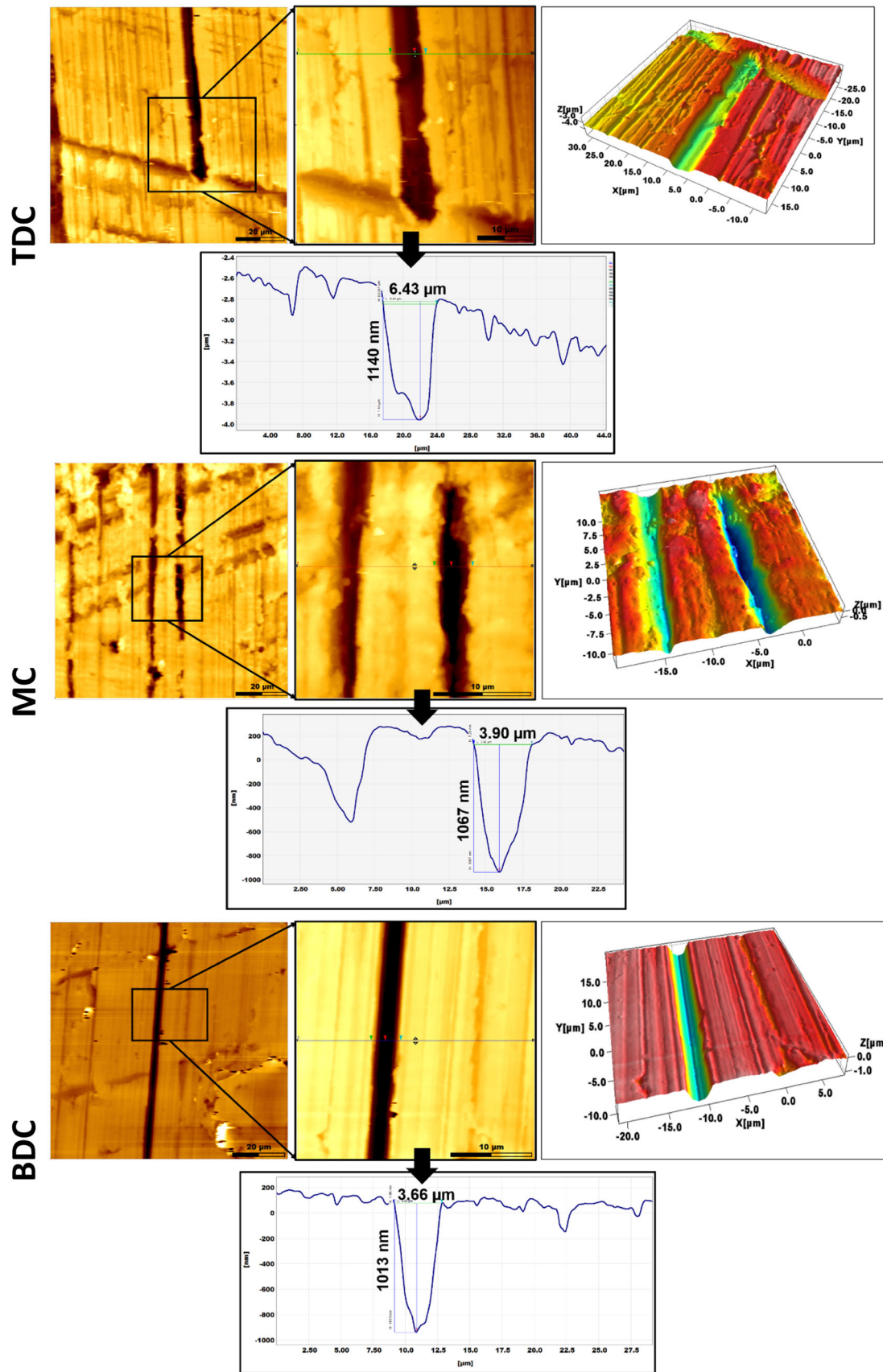


Fig. 10 AFM analysis on cylinder liner surface run with ZDDPs

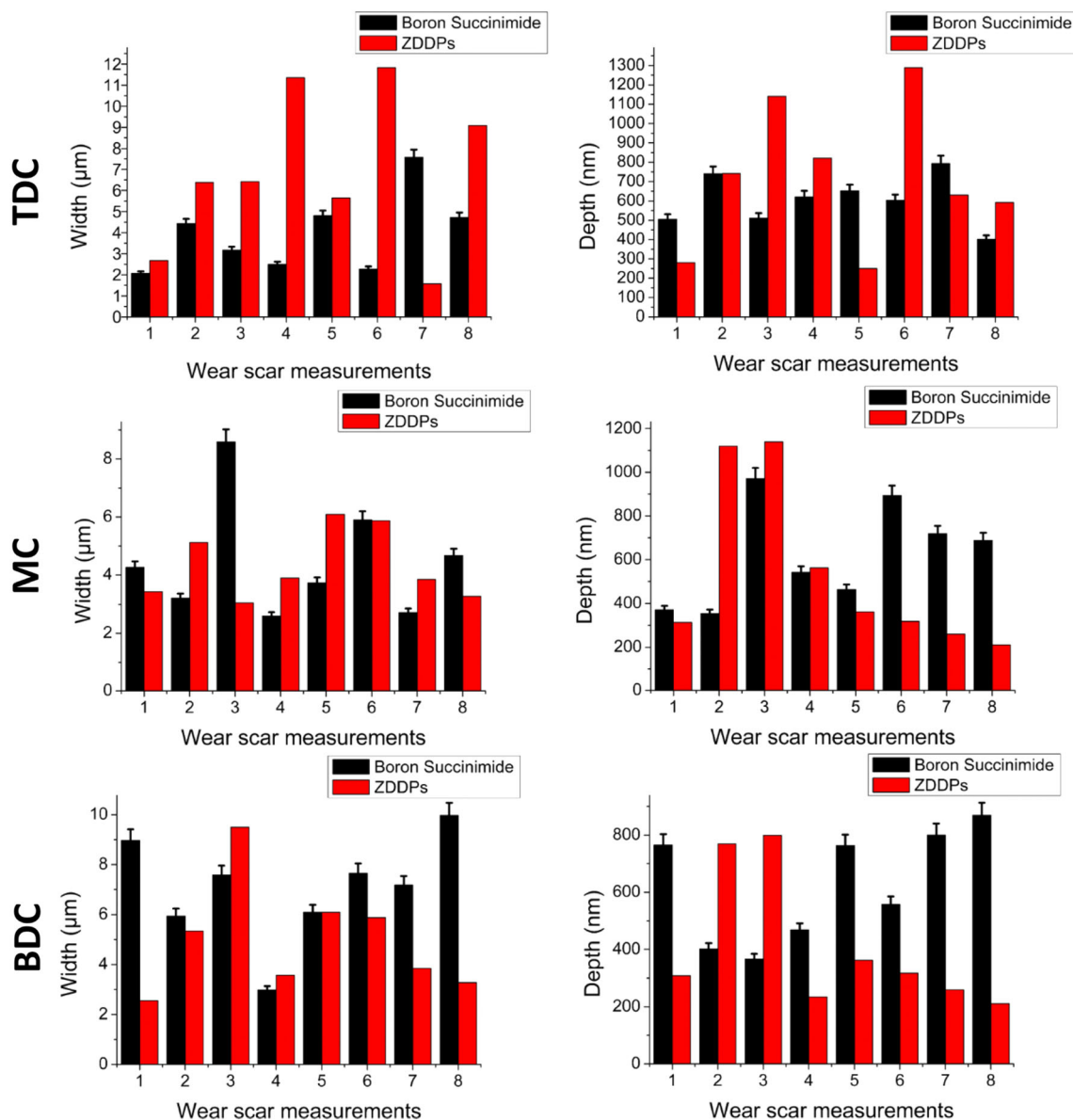


Fig. 11 Abrasive wear width and depth measurement results of 8 cylinder liners

to 95 nm (see Fig. 7f). This showed that boron succinimide formed thicker tribofilm on the ring surface than the ZDDPs. Detected boron, zinc and phosphorus quantities with XPS survey showed the density of anti-wear additives and was supported by the AFM measurements where higher density of B than Zn and P were detected.

3.2 Wear mechanisms and wear analyses on cylinder liner surfaces

3.2.1 Abrasive wear mechanism

Wear widths and depths were measured by AFM. All of the cylinder liner and ring sample surfaces were scanned with

AFM and SEM from one side to another side of the samples. At the end of the AFM analyses, the widest and deepest 8 wear scars for cylinder liners and 5 for piston rings were selected and compared to abrasive wear scar mechanism. Figure 8 shows SEM images, illustrating the abrasive wear scars which are parallel to the sliding direction of the piston at TDC of the cylinder liner run with boron succinimide anti-wear additive. Figure 8a shows an example of cutting type abrasive wear, approximately 5 µm in width which has ridges on both sides. A ploughing type abrasive wear is shown in Fig. 8b and black arrows show removed material from groove to ridges due to ploughing process. Yellow arrows in Fig. 8 show wear

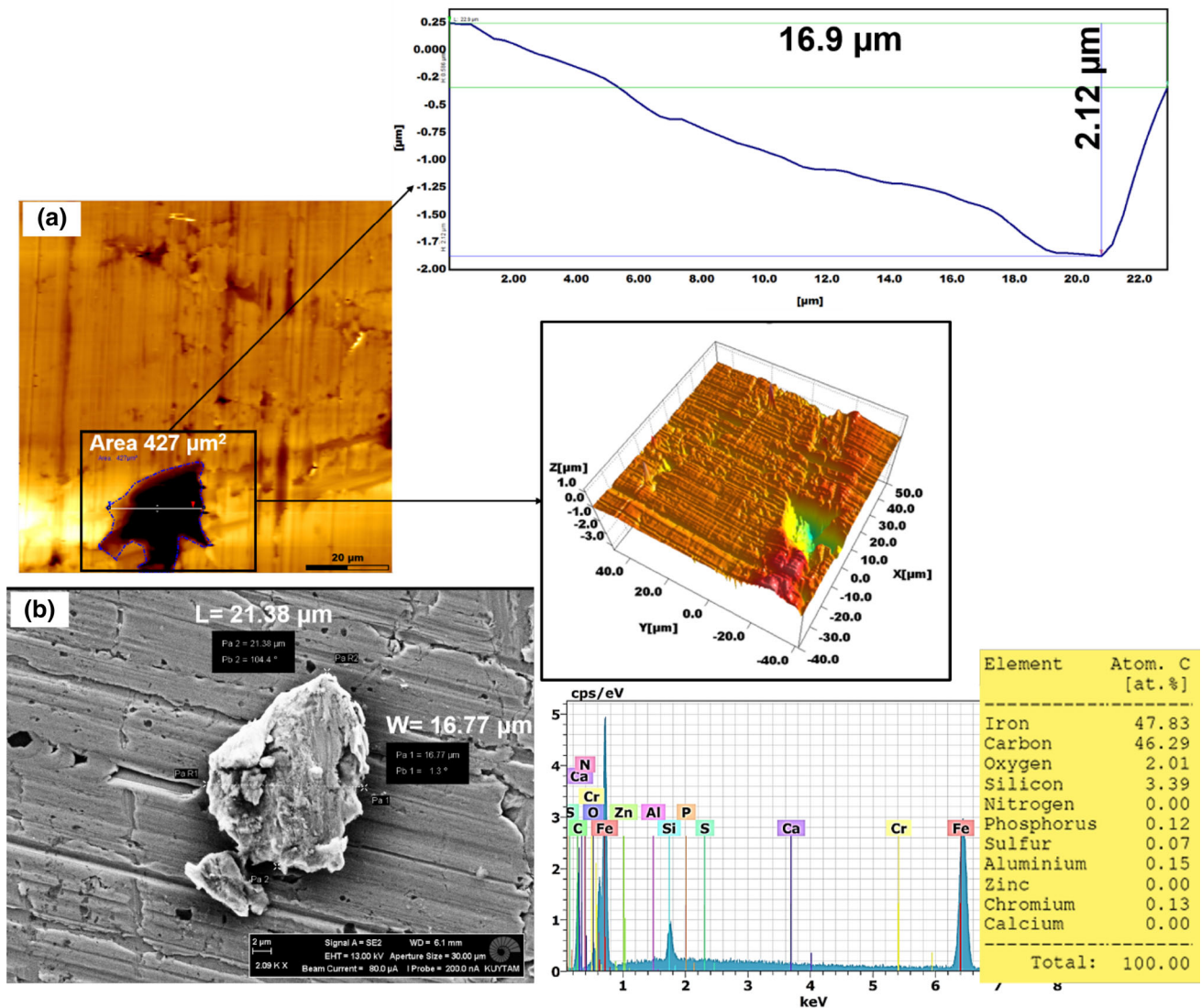


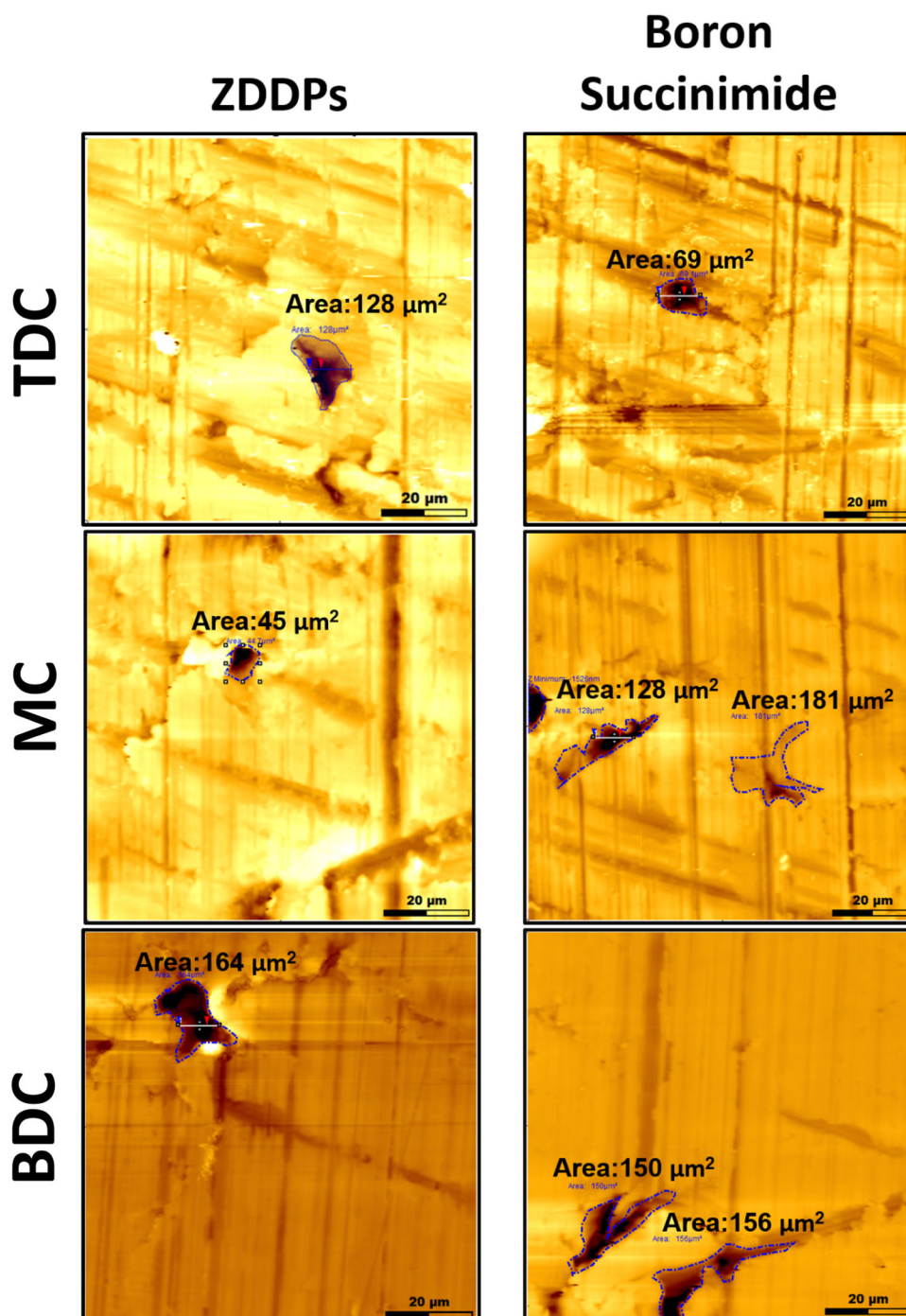
Fig. 12 The largest adhesion wear at BDC run with ZDDPs, a AFM topography image, b SEM/EDX analysis of wear particle, which left from the surface

debris on the surface after the cutting abrasion wear and adhesion wear processes.

Figure 9 shows AFM measurements of cylinder liner surface which run with boron succinimide anti-wear additive. For the TDC, a cutting type abrasive wear was observed on the surface whose depth was 794 nm and the width was 7.57 μm. At MC, depth of cutting type abrasive wear was 887 nm and width was 5.81 μm. It can be seen that wear depths and widths are bigger in cutting mode due to high scratching angle between cylinder liner and piston ring and no material displaced to the sides of the grooves. At the BDC two abrasive wear scars were shown. A ploughing type abrasive wear scar was observed as a result of the lower depth and scratching angle whose width was 6.13 μm and depth was 306 nm [25]. The measured

average width and depth of wear scars for TDC were found to be 3.94 μm and 603.6 nm for boron succinimide, respectively. At the MC, average wear scar width and depth was 4.46 μm and 625 nm, at the BDC average wear scar width was 7.04 μm and depth was 624.12 nm, respectively. Figure 10 shows AFM analyses of cylinder liner samples lubricated with ZDDPs. At the TDC of cylinder liner, wear scars were wider (width = 6.43 μm, depth = 1140 nm) and deeper than MC (width = 3.90 μm, depth = 1067 nm) and BDC (width = 3.66 μm, depth = 1013 nm). The average wear widths at TDC, MC and BDC were 5.9, 4.3, 4.98 μm, respectively (see Fig. 11). Cutting type abrasive wear scars were dominant on the cylinder liner surface which run with ZDDPs. According to the measurement results, wear widths

Fig. 13 Adhesion wear on the cylinder liner surfaces, detected by AFM measurements



increased from TDC to BDC for boron succinimide-lubricated cylinder liner (see Fig. 11). This can be explained by tribofilm formation on the surfaces where XPS surveys on tribofilm showed that boron and nitrogen concentrations decreased from TDC to BDC similarly with wear widths. This presented that load and elevated temperatures promoted faster decomposition of boron succinimide and provided richer tribofilm formation at TDC and with the decrease of load and temperature by the motion of piston

towards the BDC, induced slower boron succinimide decomposition [26].

Decomposition of boron succinimide formed intensive and strong anti-wear BN layers on tribofilm at TDC where boundary lubrication regime was dominant and BN richer tribofilm provided high wear resistance and lower level of abrasive wear widths as seen in Fig. 11. Similarly, Martin et al., Ladaviere et al., Yunbin and Pawlak reported that boron compounds can generate BN structures by

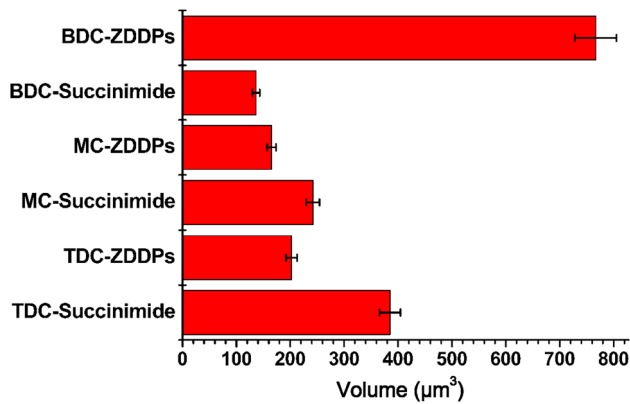


Fig. 14 Material losses of cylinder liners evaluated by AFM measurements

tribochemical reaction under boundary lubrication. During the sliding process the borate molecules are broken down, in the presence of nitrous additives, and recombine to form BN tribofilm that was similar to the results of this study [21, 27–29].

In real engine environment, when piston moved towards the BDC, load and temperature decreased and the decrease in load and temperature provided lower BN formations on the MC and BDC surfaces. Related to this situation, abrasive wear widths increased from MC to BDC surfaces when compared to TDC surface. However, on the ZDDP-lubricated cylinder liner surface wear width range was $\text{TDC} > \text{BDC} > \text{MC}$ which was similar to the literature findings [30–32]. When compared to boron ratios at TDC, MC, BDC in XPS survey, there were no such big differences between Zn, P and S. However, higher level of wear widths at TDC can be explained by the literature survey, which explains that ZDDPs grow thicker tribofilm under the highest contact pressures at TDC who is unstable. Having thicker tribofilms under higher level of load does not result in improved wear and provide lower level of wear protection [33, 34]. However, findings in this study presented opposite results for BN tribofilm formations where thicker tribofilm provided better wear resistance at TDC. Comparison of wear widths and depth results between boron succinimide and ZDDP-lubricated cylinder liners showed that BN tribofilm presented higher wear resistance than the ZDDPs at TDC and MC. When looking at the wear dimensions at BDC, ZDDPs (average wear depth was 407.9 nm) showed better results than the boron succinimide (average wear depth was 624.12 nm). Especially, there were big differences on wear depths due to lower BN formation on tribofilm that influenced the wear depths and provide higher level of wear depths where piston speed goes to zero at BDC. In general, boron succinimide formed BN tribolayers which increased

mechanochemical reactivity between sliding surfaces and these layers can be predictive of anti-wear performance [34].

3.2.2 Adhesion wear mechanism

While scanning the cylinder liner surfaces with AFM, adhesion wear mechanism was detected in different sizes and depths. Area, maximum depth and wear volume were measured and calculated by SPIP 6.6.2 software. In addition to this, total material loss (adhesion wear volume) was calculated for each cylinder liner surface. An example of detected groove on the surface of BDC whose area was $427 \mu\text{m}^2$ is shown in Fig. 12a. The depth of this groove was $2.12 \mu\text{m}$ and calculated total material loss was $371 \mu\text{m}^3$.

In addition, a removed particle detected on the BDC surface with SEM analyses, which was in similar size and shape as shown in Fig. 12b and EDX analyses confirmed that this particle was iron and removed from the BDC surface whose shape and dimensions were matched with groove detected with AFM. Figure 13 shows detected grooves on the cylinder liner surfaces with the AFM scans, which were formed by metal–metal contact of piston ring and cylinder. The highest adhesion wear occurred at BDC of the cylinder liner, which was lubricated by ZDDPs and it also shows large area of metal–metal contact under low sliding velocity (detected area was $164 \mu\text{m}^2$). When looking at the material losses (see Fig. 14), total material loss ($1134.7 \mu\text{m}^3$) was higher on the cylinder liner lubricated by ZDDP than the boron succinimide-lubricated liner ($763.9 \mu\text{m}^3$). Material loss caused by adhesion wear ranged as $\text{TDC} (385.2 \mu\text{m}^3) > \text{MC} (242.1 \mu\text{m}^3) > \text{BDC} (136.6 \mu\text{m}^3)$ for the cylinder liner which run with boron succinimide and for the ZDDP-lubricated cylinder liner adhesion wear ranged as $\text{BDC} (767 \mu\text{m}^3) > \text{TDC} (202.3 \mu\text{m}^3) > \text{MC} (165.4 \mu\text{m}^3)$. For the boron succinimide-lubricated cylinder liner, the behavior of the adhesive wear is consistent with the literature, which explains this situation as result of change in load, lubrication regimes and film thickness [35]. At the TDC, where temperature and load are higher, the tendency of ring and liner to adhere to each other increased [36]. In addition to this, sliding velocity effected adhesion behavior because when sliding speed decreases like at TDC and BDC, contact area of cylinder liner and piston ring increases exponentially which results in higher metal–metal contact and degree of adhesion especially under high load and boundary lubrication regime [37].

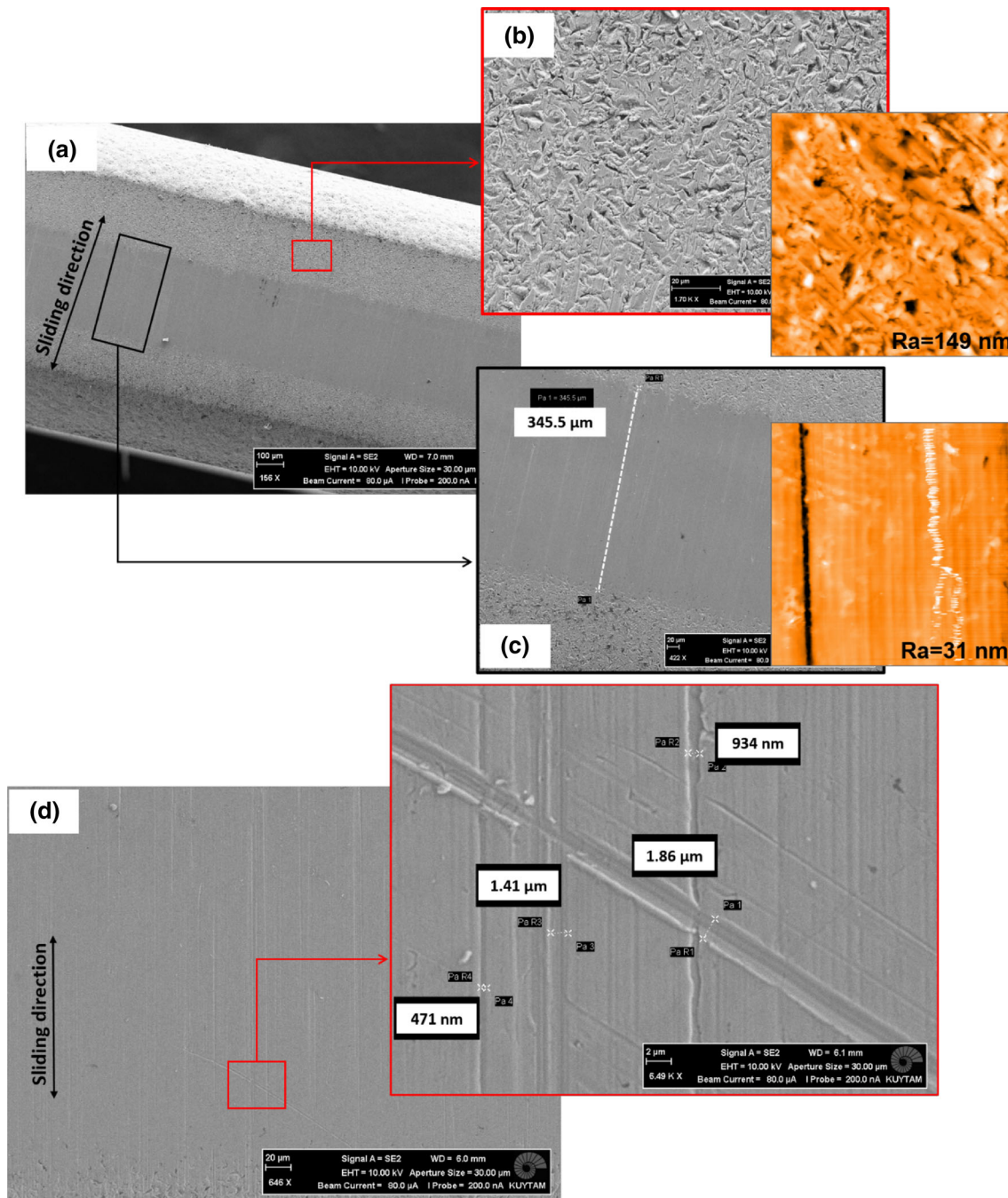
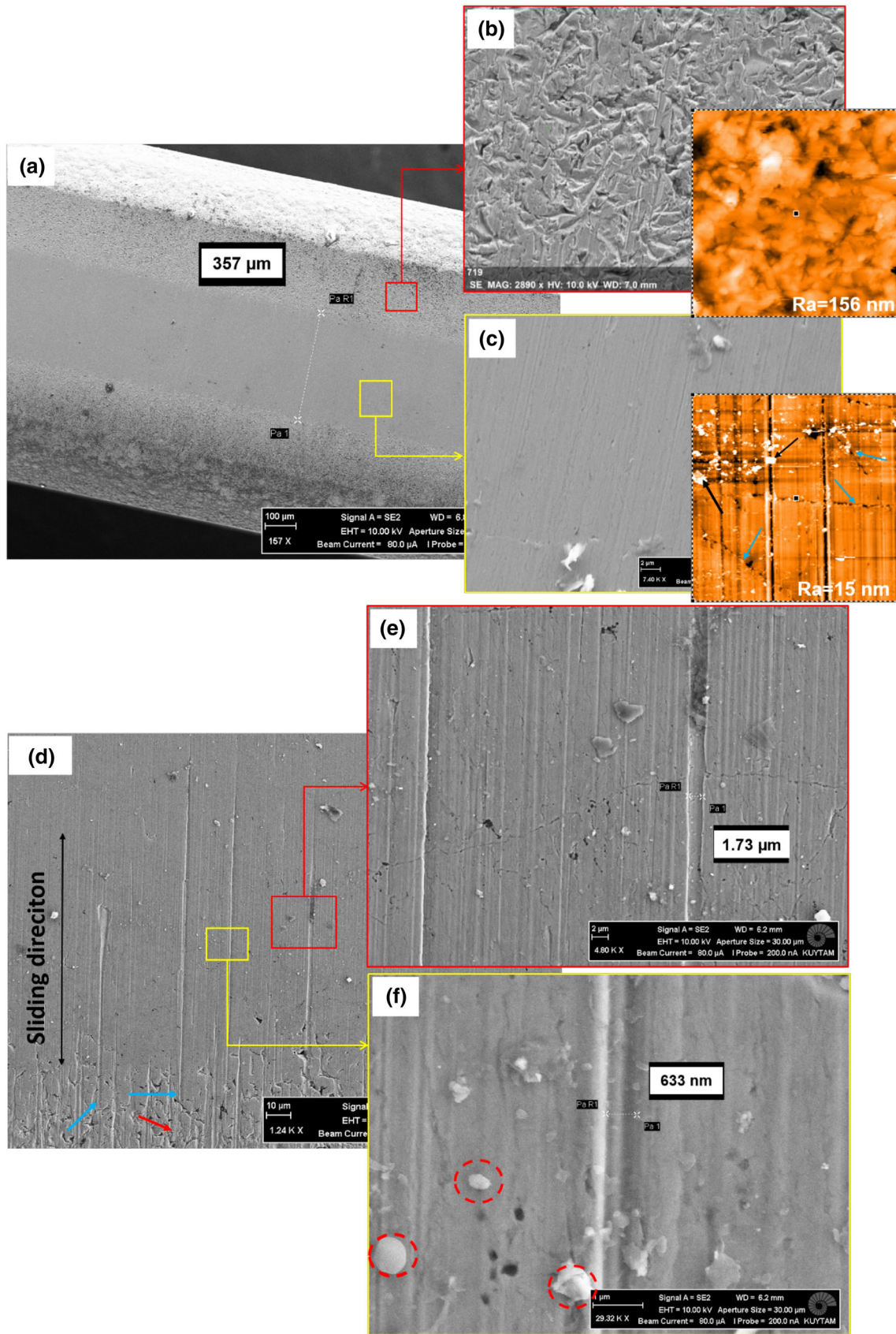


Fig. 15 Top piston ring SEM and AFM topography analyses of the engine run with boron succinimide

3.3 Wear mechanisms and wear analyses on piston ring surfaces

The chromium-coated top piston ring surfaces were analyzed at the end of the 100-h running period. Both top ring running surfaces appeared smoother at the contact areas. Figure 15 shows SEM images of the top ring run with boron succinimide and contact area of the ring (see the smoother area in Fig. 15c) was 345 μm . Non-contact area

Fig. 16 Top piston ring SEM and AFM topography analyses of the engine run with ZDDPs. **a** SEM measurement of contact region, **b** SEM and AFM topography images of non-contact area, **c** SEM and AFM topography image in which black arrows show wear particles and blue arrows show micro-cracks on the ring surface, **d** SEM image of ring surface in which red arrow shows non-contact area and blue arrows show starting point of abrasive wear scars, **e**, **f** abrasive wear scar measurements and wear particles (labeled with red circles) on the ring surface (color figure online)



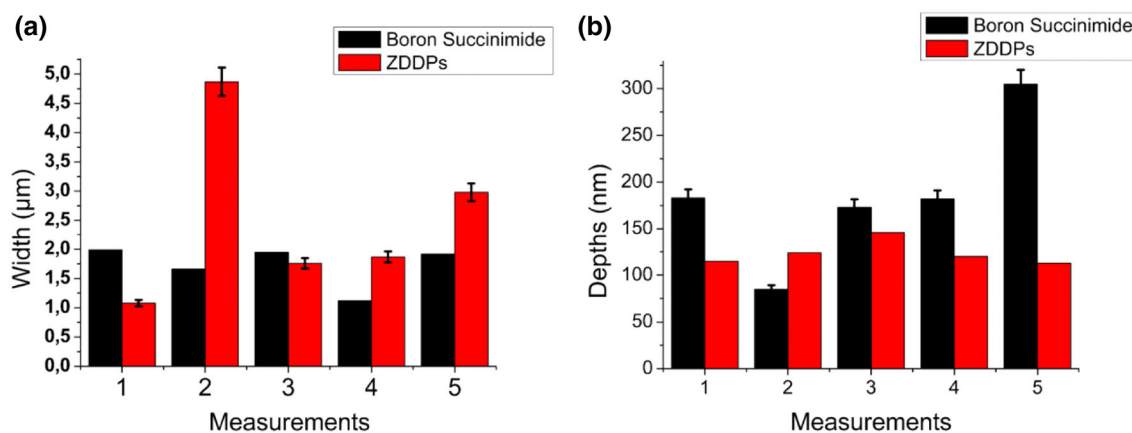


Fig. 17 Abrasive wear scar measurement results of ring surfaces by AFM, **a** wear widths, **b** wear depths

of this ring can be seen in Fig. 15b, these non-contact and contact areas were analyzed by AFM for roughness change. The average roughness of the non-contact surface (R_a) was $0.149 \mu\text{m}$ and R_a of the contact area decreased to $0.031 \mu\text{m}$. Figure 15d shows ploughing type abrasive wear mechanisms, which their widths were 0.471 , 1.4 , 1.85 and $0.93 \mu\text{m}$, respectively. The contact region width of the ring run with ZDDPs was $357 \mu\text{m}$ as it can be seen in Fig. 16a. The measured R_a of the non-contact area for ZDDP was $0.156 \mu\text{m}$ (see Fig. 16b) and R_a of the contacted surface was $0.015 \mu\text{m}$ (see Fig. 16c). In addition to wear particles (labeled with black arrows), micro-cracks (labeled with blue arrows) were detected on ring surface in AFM analyses (see Fig. 16c).

As can be seen in Fig. 16d, red arrow illustrates non-contact and unworn area, blue arrows show starting point of the abrasive wear scars. These wear scars induced by particles, which had removed from the contact area during the reciprocation motion of ring on liner as detected on the surface and these removed particles (see labeled red circles in Fig. 16f) produce three body abrasive wear scars between ring and liner surfaces. Figure 16e, f shows abrasive wear scars which are parallel to the sliding direction in 0.63 and $1.73 \mu\text{m}$ width, respectively. SEM, AFM observations and roughness measurements showed that polishing and abrasive wear formed on the contact area of the chromium-coated ring surfaces for top rings in both engines. However, according to the surface roughness changes more polishing was formed on the ZDDP-lubricated ring surface and due to the detected micro-cracks, more surface deformation occurred on the ZDDP-lubricated ring surface at similar engine running conditions.

When looking at the abrasive wear measurement results in Fig. 17, average wear width was higher on the ZDDP-lubricated ring surface (average wear width = $2.52 \mu\text{m}$) than the boron succinimide-lubricated ring (average wear width = $1.72 \mu\text{m}$). However, in average, wear depth for

piston ring surface which ran with ZDDPs was 124 nm and with boron succinimide was 186 nm where the difference between two ring surfaces was approximately 80 nm . Lower polishing and abrasive wear scar widths for boron succinimide-lubricated ring can be attributed to tribofilm thickness that was higher than the ZDDP-formed tribofilm and higher BN wear resistance. Engine tests for the two additive packages were performed with same test procedures which were covered by ISO standard. Area and volume measurements were calculated by SPIP 6.6.2 software sensitively and with great accuracy. It is not needed to perform uncertainty analysis due to no use of any equation in our analysis results.

Generally, comparison of surface analyses results show that abrasive wear is the common wear mechanism for ZDDPs and boron succinimide anti-wear additive on cylinder liners and piston ring surfaces at similar engine running conditions. Results showed that boron succinimide had better anti-wear performance than the ZDDPs for protecting the cylinder liner surfaces against the adhesive wear and material loss in engine bench tests. Similarly, it provided better wear protection in the light of polishing and abrasive wear mechanisms for top piston rings. In addition, tribochemical analyses presented that boron succinimide formed strong anti-wear tribofilms on the surfaces and it protected surfaces against wear. It is important to evaluate boron succinimide anti-wear efficiency in real engine environment and this study presents that boron succinimide can provide anti-wear tribofilms and protect the sliding surfaces against the wear.

4 Conclusions

The anti-wear performance, including tribofilm formation and wear mechanisms of boron succinimide and ZDDP anti-wear additives were evaluated by engine bench tests

and surface analyses. Based on the engine bench tests and microscopic, spectroscopic analyses results, the conclusions of this study can be summarized as follows:

- On both surfaces, tribofilms formed like pads for both anti-wear additives.
- PO and ZnP chemical compounds formed on the surfaces for ZDDPs and boron succinimide formed BN tribolayers on the surfaces.
- Dominant wear mechanism was abrasive wear for both surfaces. Although abrasive wear widths were higher at TDC for ZDDPs, lower at TDC for succinimide due to intensive decomposition under higher load, temperature and BN formations.
- Observed adhesive wear and plastic deformations with the removed wear particles were higher on the cylinder liner on ZDDPs lubricated surface.
- Polishing was observed for both piston rings with line contact in similar dimensions and polishing was higher on ring surface run with ZDDPs than the ring surface run with boron succinimide.

The results presented in this study showed that boron succinimide can be an alternative anti-wear additive considering its anti-wear performance in real engine environment from the perspective of anti-wear efficiency.

Acknowledgements The authors would like to thank the Dr. Hiroshi Fujita for their oil support in this work from Idemitsu Kosan Co. Ltd. petrochemical company in Japan, Dr. Oğuzhan GÜRLÜ from Istanbul Technical University for AFM supports and Dr. Barış YAĞCI from Koç University Surface Science and Technology Centre for chemical analyses.

References

1. Bhushan B (2001) Diesel engine tribology, modern tribology handbook, vol 1. CRC Press, Boca Raton, pp 1233–1246
2. Dresel W, Mang T (2007) Lubricants and lubrication. Wiley, Weinheim, pp 108–109
3. Barnes AM, Bartle KD, Thibon VRA (2001) A review of zinc dialkyldithiophosphates (ZDDPs): characterisation and role in the lubricating oil. *Tribol Int* 34:389–395
4. Mortier RM, Fox MF, Orszulik ST (2010) Chemistry and technology of lubricants, 3rd edn. Springer, Berlin
5. Spikes H (2004) History and mechanisms of ZDDP. *Tribol Lett* 17(3):469–489
6. Pereira G, Lachenwitzer A, Nicholls MA, Kasrai M, Norton PR, Stasio GD (2005) Chemical characterization and nanomechanical properties of antiwear films fabricated from ZDDP on a near hypereutectic Al–Si alloy. *Tribol Lett* 18(4):411–414
7. Schneider A, Brenner J, Tomastik C, Franek F (2010) Capacity of selected ionic liquids as alternative EP/AW additive. *Lubr Sci* 22:215–223
8. Yan L, Yue W, Wang C, Wei D, Xu B (2012) Comparing tribological behaviors of sulfur- and phosphorus-free organomolybdenum additive with ZDDP and MoDTC. *Tribol Int* 53:150–158
9. Minami I, Murakami H, Nanao H, Mori S (2006) Additive effect for environmental lubricants-decreased phosphorus contents in low viscosity base oils for antiwear performance. *J Jpn Pet Inst* 49:268–273
10. Wilkins AJJ, Hannington NA (1990) The effect of fuel and oil additives on automobile catalyst performance. *Platin Met* 34:16–24
11. Katafuchi T, Shimizu N (2007) Evaluation of the antiwear and friction reduction characteristics of mercaptocarboxylate derivatives as novel phosphorus-free additives. *Tribol Int* 40:1017–1024
12. <http://www.oilspecifications.org>. Accessed 12 May 2016
13. Service Fill Oils For Gasoline Engines Light Duty Diesel Engines (2012) Engines with aftertreatment devices and heavy duty diesel engines. ACEA European Oil Sequences, Bruxelles
14. Inoue K, Kurahashi T, Negishi T, Akiyama K, Arimura K, Tasaka K (1992) Effects of phosphorus and ash contents of engines on deactivation of monolithic three-way catalysts and oxygen sensors, SAE 920654
15. Mortier RM, Fox MF, Orszulik ST (2010) Chemistry and technology of lubricants, 3rd edn. Springer, New York, pp 100–110
16. Pawlak Z (2003) Tribochemistry of lubrication oils. *Tribology and interface engineering series*, no. 45. Elsevier, Amsterdam
17. Barros MID, Bouchet J, Raoult I, Mogne TL, Martin JM, Kasrai M, Yamada Y (2003) Friction reduction by metal sulfides in boundary lubrication studied by XPS and XANES analyses. *Wear* 254:863–887
18. Stepina V, Vesely V (1992) Lubricants and special fluids, tribology series. Elsevier, Slovakia, pp 318–325
19. Gosvami NN, Bares JA, Mangolini F, Konicek AR, Yablon DG, Carpick RW (2015) Mechanisms of antiwear tribofilm growth revealed in situ by single-asperity sliding contacts. *Science* 348:102–106
20. Shah UF, Glavatskih S, Antzutkin ON (2013) Boron in tribology: from borates to ionic liquids. *Tribol Lett* 51:281–301
21. Junbin Y (1997) Antiwear function and mechanism of borate containing nitrogen. *Tribol Int* 30:387–389
22. Barrell DJW, Priest M, Taylor CM (2004) Experimental simulation of impact and sliding wear in the top piston ring groove of a gasoline engine. *J Eng Tribol* 218:173–183
23. Varlot K, Martin JM, Grossiord C, Vargiolu R, Vacher B, Inoue K (1999) A dual-analysis approach in tribochemistry: application to ZDDP/calcium borate additive interactions. *Tribol Lett* 6:181–189
24. Unnikrishnan R, Jain MC, Harinarayan AK, Mehta AK (2002) Additive–additive interaction: a XPS study of the effect of ZDDP on the AW/EP characteristics of molybdenum based additives. *Wear* 252:240–249
25. Hokkiriwaga K, Kato K (1988) The effects of hardness on the transition of the abrasive wear mechanism of steels. *Wear* 123:241–251
26. Komvopoulos K, Do V, Yamaguchi ES, Yeh SW, Ryason PR (2004) X-ray photoelectron spectroscopy analyses of antiwear tribofilms produced on boundary-lubricated steel surfaces from sulfur- and phosphorus-containing additives and metal deactivator additive. *Tribol Trans* 47:321–327
27. Martin JM, LeMogne Th, Chassagnette C, Grades MN (1992) Friction of hexagonal boron nitride in various environments. *Tribol Trans* 35:462–472
28. Ladaviere R, Martin JM, LeMogne Th, Vacher B, Constans B, Iovine S (2003) Tribochemistry: friction-induced lamellar solids from lubricant additives. *Tribol Res Des Eng Syst Tribol Ser* 41:15–22
29. Pawlak Z, Kaldonski T, Paid R, Bayraktar E, Oloyede E (2009) A comparative study on the tribological behaviour of hexagonal

- boron nitride (h-BN) as lubricating micro-particles: an additive in porous sliding bearings for a car clutch. *Wear* 267:1198–1202
30. Ali SHR, Mohamed HH, Bedewy MK (2009) Int J Precis Eng Manuf 10:19
 31. Rosen BG, Ohlsson R, Thomas TR (1996) Wear of cylinder bore microtopography. *Wear* 198:271–279
 32. Srivastava DK, Agarwal AK, Kumar J (2007) Effect of liner surface properties on wear and friction in a non-firing engine simulator. *Mater Des* 28:1632–1640
 33. Yablon DG, Kalamaras PH, Deckman DE, Webster MN (2006) Atomic force microscopy and raman spectroscopy investigation of additive interactions responsible for anti-wear film formation in a lubricated contact. *Tribol Trans* 49:108–116
 34. Konicek AR, Jacobs PW, Webster MN, Schilowitz AM (2016) Role of tribofilms in wear protection. *Tribol Int* 94:14–19
 35. Kimura Y, Wakabayashi T, Okada K, Wada T, Nishikawa H (1999) Boron nitride as a lubricant additive. *Wear* 232:199–206
 36. Sargent LB Jr (1978) On the fundamental nature of metal–metal adhesion. *SLE Trans* 21(4):285–290
 37. Arakawa K (2015) Effects of wear on contact area and dynamic sliding velocity. *Wear* 328:552–555